

Materials and Methods

Cell culture and reagents

The *EGFR* mutant NSCLC cell lines HCC827 (del E746_A750) and the human glioblastoma cell line U87MG were obtained from the American Type Culture Collection. HCC827 GR5 (del E746_A750/*MET* amplified) was generated and characterized as described previously (6). We screened all sublines of HCC827 for the presence of *EGFR* mutations by direct DNA sequencing of exons 18 to 21 and *MET* amplification by fluorescence *in situ* hybridization analysis with a probe specific for *MET* and a control probe for the centromere of chromosome 7 as described previously (19, 20) for this study. All cells were passaged for ≤ 3 months before the renewal from frozen, early-passage stocks obtained from the indicated sources. Cells were regularly screened for mycoplasma with the use of a MycoAlert Mycoplasma Detection Kit (Lonza). HCC827 cells were cultured under a humidified atmosphere of 5% CO₂ at 37°C in RPMI 1640 medium (Sigma) supplemented with 10% fetal bovine serum. HCC827 GR5 cells were cultured in RPMI 1640 medium supplemented with 10% fetal bovine serum and 1 $\mu\text{mol/L}$ gefitinib. U87MG cells were cultured in DMEM (Gibco) supplemented with 10% fetal bovine serum. TAK-701 was kindly provided by Takeda Pharmaceutical Co. Ltd., gefitinib was obtained from AstraZeneca, and PHA-665752 was from Tocris Bioscience.

Cell transfection

A full-length cDNA fragment encoding human HGF was obtained from U87MG cells by reverse transcription and PCR with the primers HGF-F (5-GCGGCCGCGAG-CACCATGTGGGTGACCAAA-3) and HGF-R (5-CGGGATCCCTAIGACTGTGGTACCTTATAT-3). The amplification product was verified by sequencing after its cloning into the pCR-Blunt II-TOPO vector (Invitrogen). The HGF cDNA was excised from pCR-Blunt II-TOPO and transferred to the pQCXIH retroviral vector (Clontech). Retroviruses encoding HGF were then produced and used to infect HCC827 cells as described

(21). Cells stably expressing HGF were then isolated by selection with hygromycin at 500 $\mu\text{g/mL}$ (InvivoGen).

Enzyme-linked immunosorbent assay for HGF

Cells (5×10^5) were seeded in 6-well plates, cultured overnight in complete medium, and then incubated in serum-free medium for 24 hours, after which the latter medium was collected and assayed for HGF with a Human HGF Quantikine ELISA Kit (R&D Systems). A standard curve for the enzyme-linked immunosorbent assay (ELISA) was generated with the supplied reagents, and HGF concentration was determined as the average value from triplicate samples.

Cell growth inhibition assay

Cells were transferred to 96-well flat-bottomed plates and cultured for 24 hours before exposure for 72 hours to various concentrations of gefitinib, TAK-701, or PHA-665752, as indicated. Tetra Color One (5 mmol/L tetrazolium monosodium salt and 0.2 mmol/L 1-methoxy-5-methyl phenazineium methylsulfate; Seikagaku Kogyo) was then added to each well, and the cells were incubated for 3 hours at 37°C before measurement of absorbance at 490 nm with a Multiskan Spectrum instrument (Thermo Labsystems). Absorbance values were expressed as a percentage of that for untreated cells.

Annexin V binding assay

The binding of Annexin V to cells was measured with the use of an Annexin-V-FLUOS Staining Kit (Roche). Cells were harvested by exposure to trypsin-EDTA, washed with PBS, and centrifuged at 200 $\times g$ for 5 minutes. The cell pellets were resuspended in 100 μL of Annexin-V-FLUOS labeling solution, incubated for 10 to 15 minutes at 15°C to 25°C, and then analyzed for fluorescence with a flow cytometer (FACS-Calibur) and Cell Quest software (Becton Dickinson).

Immunoblot analysis

Cells were washed twice with ice-cold PBS and then lysed with 1 \times cell lysis buffer (Cell Signaling Technology) consisting of 20 mmol/L Tris-HCl (pH 7.5), 150 mmol/L NaCl, 1 mmol/L EDTA (disodium salt), 1 mmol/L EGTA, 1% Triton X-100, 2.5 mmol/L sodium pyrophosphate, 1 mmol/L β -glycerophosphate, 1 mmol/L Na₂VO₄, leupeptin (1 $\mu\text{g/mL}$), and 1 mmol/L phenylmethylsulfonyl fluoride. The protein concentration of cell lysates was determined with a bicinchoninic acid protein assay kit (Thermo Fisher Scientific), and equal amounts of protein were subjected to SDS-PAGE on 7.5% gels (Bio-Rad). The separated proteins were transferred to a nitrocellulose membrane, which was then incubated with Blocking One solution (Nacalai Tesque) for 20 minutes at room temperature before incubation overnight at 4°C with primary antibodies. Antibodies to phosphorylated EGFR (phosphotyrosine-1068), to phosphorylated MET (phosphotyrosine-1349), to phosphorylated or total forms

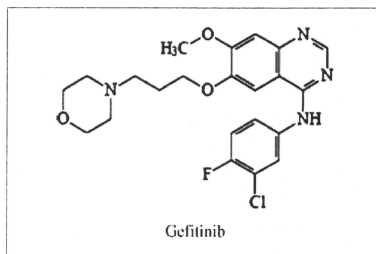


Figure 1. The structure of gefitinib.

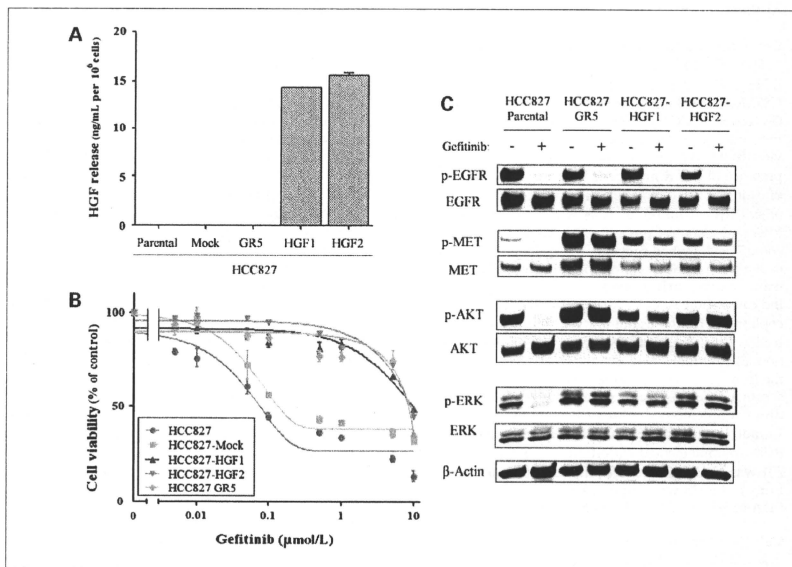


Figure 2. Characterization of HCC827 isogenic cell lines. A, HCC827 isogenic cell lines (HCC827, HCC827-Mock, HCC827-HGF1 and -HGF2, and HCC827-GRS) were cultured overnight in medium containing 10% serum and then incubated for 24 hours in serum-free medium, after which the culture supernatants were collected and assayed for HGF with an ELISA. Data are means \pm SD from three independent experiments. B, HCC827 isogenic cell lines were cultured in medium containing 10% serum for 72 hours in the presence of various concentrations of gefitinib, after which cell viability was assessed as described in Materials and Methods. The number of viable cells is expressed as a percentage of the value for untreated cells. Data are means \pm SD from three independent experiments. C, HCC827 isogenic cell lines were incubated for 1 hour with or without gefitinib (100 nmol/L) in medium containing 10% serum, after which the cells were lysed and subjected to immunoblot analysis with antibodies to phosphorylated (p-) or total forms of EGFR, MET, AKT, or ERK, or with those to β -actin (loading control).

of AKT, and to phosphorylated extracellular signal-regulated kinase (ERK) were obtained from Cell Signaling Technology; those to total ERK were from Santa Cruz Biotechnology; those to total EGFR and to total MET were from Zymed/Invitrogen; and those to β -actin were from Sigma. The membrane was then washed with PBS containing 0.05% Tween 20 before incubation for 1 hour at room temperature with horseradish peroxidase-conjugated secondary antibodies (GE Healthcare). Immune complexes were finally detected with ECL Western blotting detection reagents (GE Healthcare).

Growth inhibition assay *in vivo*

All animal studies were done in accordance with the Recommendations for Handling of Laboratory Animals for Biomedical Research compiled by the Committee on Safety and Ethical Handling Regulations for Laboratory Animal Experiments, Kinki University. The ethical proce-

dures followed met the requirements of the United Kingdom Coordinating Committee on Cancer Research guidelines (22). HCC827 cells were implanted s.c. into the right hind leg of 6-week-old female athymic nude mice (BALB/c *nu/nu*; CLEA Japan). Tumor volume was determined from caliper measurement of tumor length (*L*) and width (*W*) according to the formula $LW^2/2$. Treatment was initiated when tumors in each group of animals achieved an average volume of 300 to 400 mm³. Treatment groups (each containing five mice) consisted of vehicle control, TAK-701 alone, gefitinib alone, and TAK-701 plus gefitinib. The mice were injected with TAK-701 (5 mg/kg) i.p. twice a week for 7 weeks; control animals received PBS as vehicle. Gefitinib (50 mg/kg) was administered by oral gavage daily for 49 days; control animals received a 0.5% (w/v) aqueous solution of hydroxypropylmethylcellulose as vehicle. Both tumor size and body weight were measured twice per week.

Statistical analysis

The data, presented as means \pm SD or SE, were analyzed with Student's two-tailed *t* test, with *P* < 0.05 considered statistically significant.

Results

Cell-derived HGF induces gefitinib resistance in EGFR mutation-positive NSCLC cells

To investigate whether cell-derived HGF induces gefitinib resistance in NSCLC cells with an *EGFR* mutation, we established HCC827 cells (which are *EGFR* mutation positive) that stably express human HGF (HCC827-HGF1 and -HGF2 cells) or stably harbor the corresponding empty vector (HCC827-Mock cells). The secretion of HGF from these cell lines as well as from the parental (HCC827) cells and from an HCC827 subline with *MET* amplification (HCC827 GR5) was examined with the use of an ELISA. We found that HCC827-HGF1 and -HGF2 cells released large amounts of HGF into the culture medium, whereas the secretion of HGF from parental

(HCC827), HCC827-Mock, or HCC827 GR5 cells was undetectable (Fig. 2A). To assess the effects of gefitinib on cell growth, we exposed these five cell lines to various concentrations of the drug and then measured cell viability. HCC827 GR5 as well as HCC827-HGF1 and -HGF2 cells showed a reduced sensitivity to gefitinib compared with HCC827 and HCC827-Mock cells, with median inhibitory concentrations of \sim 10 μ M/L apparent for the former cell lines compared with \sim 0.1 μ M/L for the latter (Fig. 2B). To investigate possible differences in signal transduction among these cell lines, we examined the effects of gefitinib on *EGFR*, *MET*, *AKT*, and *ERK* phosphorylation by immunoblot analysis (Fig. 2C). In the parental cells, gefitinib markedly inhibited the phosphorylation of *EGFR*, *AKT*, and *ERK*. In contrast, in the resistant cells (HCC827 GR5, and HCC827-HGF1 and -HGF2), gefitinib alone had no effect on *AKT* and *ERK* phosphorylation, although it substantially reduced the level of *EGFR* phosphorylation. These data suggest that sustained *AKT* and *ERK* signaling in the presence of gefitinib contributes to gefitinib

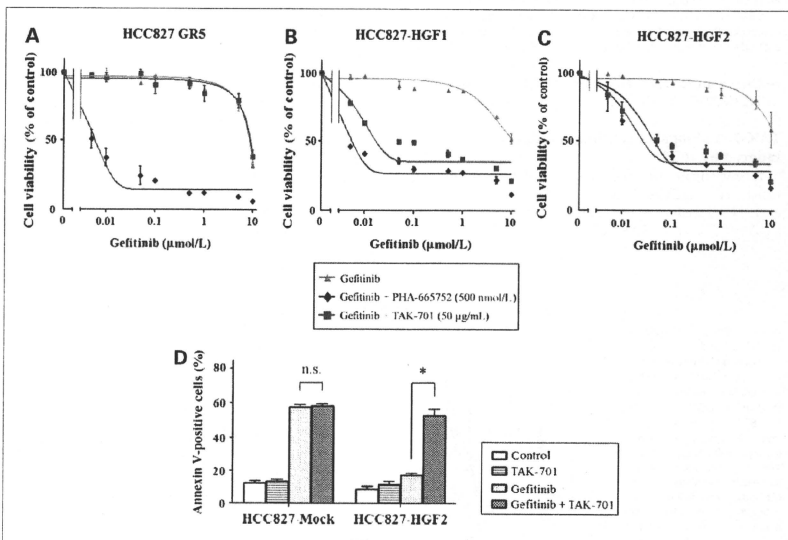


Figure 3. Effects of the combination of gefitinib and either TAK-701 or PHA-665752 on the growth of gefitinib-resistant NSCLC cells. A to C, HCC827 GR5 cells (A), HCC827-HGF1 cells (B), and HCC827-HGF2 cells (C) were cultured for 72 hours in medium containing 10% serum, various concentrations of gefitinib, and either PHA-665752 (500 nmol/L) or TAK-701 (50 μ g/mL), after which cell viability was assessed. Data are means \pm SD from three independent experiments. D, HCC827-Mock or HCC827-HGF2 cells were incubated in the absence or presence of gefitinib (1 μ M/L) or TAK-701 (50 μ g/mL) for 48 hours in medium containing 10% serum. The proportion of apoptotic cells was then assessed by staining with Annexin V followed by flow cytometry. Data are means \pm SD from three independent experiments. **P* < 0.001; n.s., not significant.

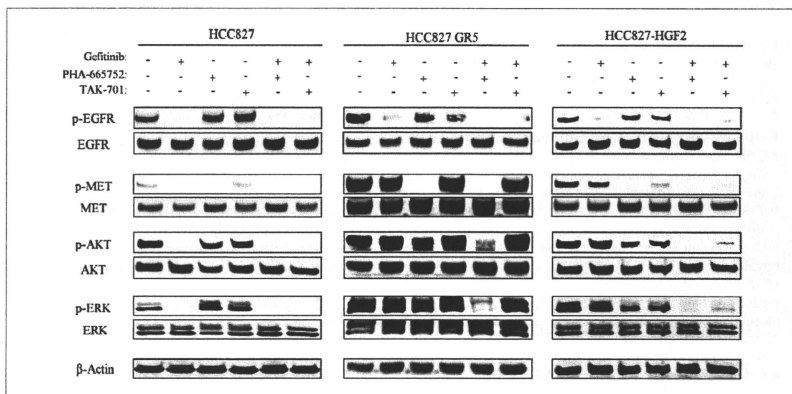


Figure 4. Effects of the combination of gefitinib and either TAK-701 or PHA-665752 on cell signaling in gefitinib-resistant NSCLC cells. HCC827 cells, HCC827 GR5 cells, and HCC827-HGF2 cells were incubated for 6 hours in medium containing 10% serum in the absence or presence of gefitinib (1 $\mu\text{mol/L}$), PHA-665752 (500 nmol/L), or TAK-701 (50 $\mu\text{g/mL}$), as indicated. Cell lysates were then prepared and subjected to immunoblot analysis with antibodies to phosphorylated or total forms of EGFR, MET, AKT, or ERK, or with those to β -actin.

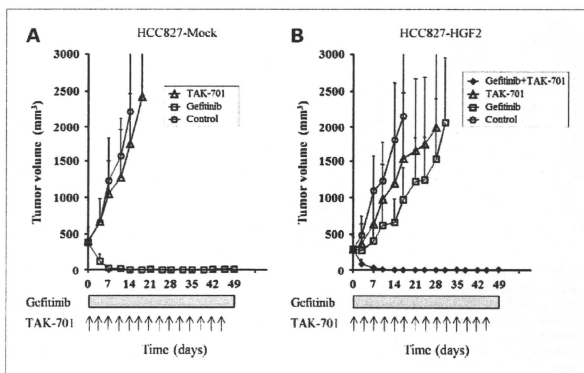
resistance in HCC827-HGF1 and -HGF2 cells as well as in HCC827 GR5 cells.

TAK-701 abrogates gefitinib resistance induced by HGF

To investigate the roles of MET and HGF in gefitinib resistance in HCC827 GR5 as well as in HCC827-HGF1 and -HGF2 cells, we exposed the cells to the MET-TKI PHA-665752 or to TAK-701, a humanized monoclonal

antibody to HGF, in combination with gefitinib. Combined treatment with PHA-665752 and gefitinib was previously shown to result in substantial growth inhibition in HCC827 GR5 (*MET* amplification-positive) cells (6). We found that the combination of gefitinib and TAK-701 did not affect the growth of HCC827 GR5 cells (Fig. 3A). In HCC827-HGF1 and -HGF2 cells, however, TAK-701 and PHA-665752 each restored the sensitivity of cell growth to inhibition by gefitinib (Fig. 3B and C).

Figure 5. Effects of the combination of TAK-701 and gefitinib on the growth of gefitinib-resistant NSCLC cells *in vivo*. Nude mice with tumor xenografts established by s.c. injection of HCC827-Mock (A) or HCC827-HGF2 (B) cells were treated for 7 weeks with vehicle (control), gefitinib (50 mg/kg), TAK-701 (5 mg/kg), or both drugs, as described in Materials and Methods. Tumor volume was determined at the indicated times after the onset of treatment. Data are means \pm SE from five mice per group. $P < 0.001$ for comparison of gefitinib versus gefitinib plus TAK-701 in B.



In addition, staining with Annexin V revealed that gefitinib alone induced a marked increase in the frequency of apoptosis in HCC827-Mock cells but elicited a much smaller effect in HCC827-HGF2 cells (Fig. 3D). However, treatment with both gefitinib and TAK-701 triggered an increase in the number of Annexin V-positive HCC827-HGF2 cells similar in extent to that induced by gefitinib alone in HCC827-Mock cells. These results thus indicate that TAK-701 restores gefitinib-induced apoptosis in HCC827-HGF2 cells.

To examine the effects of gefitinib, PHA-665752, and TAK-701 on cell signaling in the parental, HCC827 GR5, and HCC827-HGF2 cell lines, we again did immunoblot analysis (Fig. 4). Consistent with previous observations (6), PHA-665752 in combination with gefitinib inhibited MET, AKT, and ERK phosphorylation in HCC827 GR5 cells. We further found that TAK-701 alone did not inhibit MET phosphorylation, and thus the combination of TAK-701 and gefitinib did not abrogate AKT and ERK phosphorylation in HCC827 GR5 cells. In HCC827-HGF2 cells, however, TAK-701 as well as PHA-665752 inhibited MET phosphorylation, and the combined treatment with TAK-701 and gefitinib fully suppressed ERK and AKT phosphorylation. These results indicate that HGF-induced gefitinib resistance is mediated by HGF-MET signaling and is abrogated by treatment with TAK-701 in HCC827-HGF cells.

Cell-derived HGF induces gefitinib resistance in NSCLC cells and TAK-701 restores the sensitivity of tumor growth to inhibition by gefitinib *in vivo*

To examine the possible induction of gefitinib resistance by tumor cell-derived HGF and the efficacy of combined treatment with TAK-701 and gefitinib *in vivo*, we generated xenografts in nude mice by injection of HCC827-Mock or HCC827-HGF2 cells. We found that, whereas gefitinib markedly inhibited the growth of HCC827-Mock xenografts (Fig. 5A), HCC827-HGF2 xenografts were substantially resistant to gefitinib (Fig. 5B). TAK-701 alone had a minimal effect on tumor growth in both HCC827-Mock and HCC827-HGF2 xenograft models. However, the combination of gefitinib and TAK-701 induced marked regression of HCC827-HGF2 xenografts. These results thus suggest that HGF produced by NSCLC tumors harboring an *EGFR* mutation induces gefitinib resistance, and that TAK-701 abrogates such HGF-induced gefitinib resistance *in vivo*.

Discussion

In the present study, we established HGF-overexpressing sublines of HCC827 cells and showed that these sublines are resistant to gefitinib both *in vitro* and *in vivo*. To investigate whether the resistance of HCC827-HGF cells to gefitinib is attributable to HGF-MET signaling, we examined the effects of the MET-TKI PHA-665752 and of TAK-701, a humanized monoclonal antibody to HGF, on signal transduction and cell growth. In both HCC827-HGF1 and

-HGF2 cells as well as in HCC827 GR5 cells, which are positive for *MET* amplification, gefitinib alone did not inhibit AKT or ERK phosphorylation, whereas gefitinib in combination with PHA-665752 markedly suppressed the phosphorylation of these signaling molecules. Consistent with these results, PHA-665752 restored the sensitivity of cell growth to inhibition by gefitinib in HCC827-HGF cells as well as in HCC827 GR5 cells. These results indicate that the gefitinib resistance of these cell lines is mediated by MET signaling. TAK-701 has been shown to potently inhibit HGF binding to MET in cancer cells and xenograft models dependent on autocrine HGF-MET signaling.⁶ TAK-701 did not inhibit the phosphorylation of MET in HCC827 GR5 cells, suggesting that the activation of MET in these cells is not dependent on HGF. Indeed, we were not able to detect the secretion of HGF from HCC827 GR5 cells. In contrast, TAK-701 suppressed MET phosphorylation, and thus the combination of TAK-701 and gefitinib markedly inhibited both AKT and ERK signaling in HCC827-HGF cells, resulting in their growth inhibition. These results indicate that autocrine HGF-MET signaling contributes to gefitinib resistance in HCC827-HGF cells. Similar ligand-mediated gefitinib resistance has been described previously, with insulin-like growth factor having been found to rescue cells expressing wild-type *EGFR* from gefitinib-induced inhibition of cell growth (23). These observations suggest that ligand-dependent receptor tyrosine kinase (RTK) activation (by HGF or insulin-like growth factor), as well as ligand-independent RTK activation (by *MET* amplification), plays a pivotal role in the development of resistance to gefitinib. Further studies should reveal whether other ligand-RTK combinations contribute to gefitinib resistance.

We found that the baseline levels of both MET expression and MET phosphorylation in HCC827-HGF cells were lower than those in HCC827 GR5 cells (Fig. 2C), whereas HCC827-HGF cells were resistant to gefitinib to the same extent as HCC827 GR5 cells *in vitro* (Fig. 2B). These results suggest that phosphorylated MET activates downstream signaling through different pathways in HCC827 GR5 and HCC827-HGF cells. MET was recently shown to signal through ERBB3 in *MET* amplification-positive NSCLC cells (6) or through Grb2-associated binder 1 (Gab1) in NSCLC cells with HGF-induced gefitinib resistance (24). Further studies are required to investigate whether the biological properties of NSCLC cells or the abilities of drugs to overcome gefitinib resistance are affected by differences in RTK downstream signaling.

In our HCC827-HGF xenograft model, we showed that HGF secreted from *EGFR* mutation-positive NSCLC cells drives tumor growth even in the presence of gefitinib, and that combination therapy with TAK-701 and gefitinib was

⁶ Kitahara O, Nishizawa S, Ito Y, Toyoda Y, Misumi Y, Sato S, Inaoka T, Kitakamp SL, Kokubo T, Hori A. TAK-701, a humanized monoclonal antibody to human hepatocyte growth factor, exhibits promising antitumor effects on multiple tumor types. In preparation.

able to greatly inhibit the growth of HCC827-HGF tumors. These results indicate that interruption of HGF-MET signaling with TAK-701 represents a powerful strategy to abrogate gefitinib resistance induced by HGF derived from tumor cells. HGF was previously shown to be expressed predominantly by adenocarcinoma cells in NSCLC specimens, although a low level of HGF staining was also apparent in stromal cells (25). Furthermore, marked expression of HGF has been detected in most lung cancers with intrinsic or acquired resistance to gefitinib (10, 26). These data suggest that our autocrine model systems based on stable overexpression of HGF are clinically relevant and should prove useful for the establishment of strategies to overcome gefitinib resistance. HGF is also produced by stromal cells of various tumor types (13, 27, 28). Indeed, HGF derived from fibroblasts injected into nude mice together with *EGFR* mutation-positive NSCLC cells induced gefitinib resistance in the NSCLC cells *in vivo* (29). Further studies are required to clarify the major source of HGF that contributes to gefitinib resistance in patients with *EGFR* mutation-positive lung cancer. Given that TAK-701 inhibits HGF binding to MET, TAK-701 may reverse gefitinib resistance induced by HGF derived not only from tumor cells but also from stromal cells.

In conclusion, we have shown that autocrine activation of MET by HGF confers resistance to gefitinib, and that

TAK-701, a humanized monoclonal antibody to HGF, restored sensitivity to gefitinib in tumors with HGF-induced gefitinib resistance. TKIs inhibit several signaling pathways and are therefore associated with a risk of high toxicity, whereas therapeutic antibodies are thought to be less toxic as a result of their high specificity. TAK-701 is currently undergoing phase I trials as a single agent in patients with advanced solid tumors, and our results now suggest that further studies of combination therapy with TAK-701 and gefitinib are warranted in NSCLC patients with HGF-induced EGFR-TKI resistance.

Disclosure of Potential Conflicts of Interest

No potential conflicts of interest were disclosed.

Grant Support

National Institute of Health R01CA135257 (P.A. Jänne) and National Cancer Institute Lung SPORE P50CA090578 (P.A. Jänne).

The costs of publication of this article were defrayed in part by the payment of page charges. This article must therefore be hereby marked advertisement in accordance with 18 U.S.C. Section 1734 solely to indicate this fact.

Received 05/25/2010; revised 08/09/2010; accepted 08/11/2010; published OnlineFirst 08/17/2010.

References

- Lynch TJ, Bell DW, Sordella R, et al. Activating mutations in the epidermal growth factor receptor underlying responsiveness of non-small-cell lung cancer to gefitinib. *N Engl J Med* 2004;350:2129-39.
- Paez JG, Janne PA, Lee JC, et al. EGFR mutations in lung cancer: correlation with clinical response to gefitinib therapy. *Science* 2004;304:1497-500.
- Pao W, Miller V, Zakowski M, et al. EGFR receptor gene mutations are common in lung cancers from "never smokers" and are associated with sensitivity of tumors to gefitinib and erlotinib. *Proc Natl Acad Sci U S A* 2004;101:13305-11.
- Kobayashi S, Boggon TJ, Dayaram T, et al. EGFR mutation and resistance of non-small-cell lung cancer to gefitinib. *N Engl J Med* 2005;352:786-92.
- Pao W, Miller VA, Politi KA, et al. Acquired resistance of lung adenocarcinomas to gefitinib or erlotinib is associated with a second mutation in the EGFR kinase domain. *PLoS Med* 2005;2:e73.
- Engelman JA, Zejnullahu K, Mitsudomi T, et al. MET amplification leads to gefitinib resistance in lung cancer by activating ERBB3 signaling. *Science* 2007;316:1039-43.
- Bean J, Brennan C, Shin JY, et al. MET amplification occurs with or without T790M mutations in EGFR mutant lung tumors with acquired resistance to gefitinib or erlotinib. *Proc Natl Acad Sci U S A* 2007;104:20932-7.
- Bottaro DP, Rubin JS, Falotto DL, et al. Identification of the hepatocyte growth factor receptor as the c-met proto-oncogene product. *Science* 1991;251:802-4.
- Naldini L, Vigna E, Narsimhan RP, et al. Hepatocyte growth factor (HGF) stimulates the tyrosine kinase activity of the receptor encoded by the proto-oncogene c-MET. *Oncogene* 1991;6:501-4.
- Yano S, Wang W, Li Q, et al. Hepatocyte growth factor induces gefitinib resistance of lung adenocarcinoma with epidermal growth factor receptor-activating mutations. *Cancer Res* 2008;68:9479-87.
- Nakamura T, Nishizawa T, Hagiya M, et al. Molecular cloning and expression of human hepatocyte growth factor. *Nature* 1989;342:440-3.
- Maulik G, Shrikhande A, Kijima T, Ma PC, Morrison PT, Salsgia R. Role of the hepatocyte growth factor receptor, c-Met, in oncogenesis and potential for therapeutic inhibition. *Cytokine Growth Factor Rev* 2002;13:41-59.
- Birchmeier C, Birchmeier W, Gherardi E, Vande Woude GF. Met, metastasis, motility and more. *Nat Rev Mol Cell Biol* 2003;4:315-25.
- Harvey P, Warn A, Newman P, Perry LJ, Ball RV, Warn RM. Immunoreactivity for hepatocyte growth factor/scatter factor and its receptor, met, in human lung carcinomas and malignant mesotheliomas. *J Pathol* 1996;180:389-94.
- Tuck AB, Park M, Sterns EE, Boag A, Elliott BE. Coexpression of hepatocyte growth factor and receptor (Met) in human breast carcinoma. *Am J Pathol* 1996;148:225-32.
- Kocchekpour S, Jeffers M, Rulong S, et al. Met and hepatocyte growth factor/scatter factor expression in human gliomas. *Cancer Res* 1997;57:5391-8.
- Danilovitch-Miagkova A, Zbar B. Dysregulation of Met receptor tyrosine kinase activity in invasive tumors. *J Clin Invest* 2002;109:883-7.
- Tsao MS, Zhu H, Glaid A, Viallet J, Nakamura T, Park M. Hepatocyte growth factor/scatter factor is an autocrine factor for human normal bronchial epithelial and lung carcinoma cells. *Cell Growth Differ* 1993;4:571-6.
- Okabe T, Okamoto I, Tamura K, et al. Differential constitutive activation of the epidermal growth factor receptor in non-small cell lung cancer cells bearing EGFR gene mutation and amplification. *Cancer Res* 2007;67:2046-53.
- Okamoto W, Okamoto I, Yoshida T, et al. Identification of c-Src as a potential therapeutic target for gastric cancer and of MET activation as a cause of resistance to c-Src inhibition. *Mol Cancer Ther* 2010;9:1188-97.

21. Tanaka K, Arai T, Maegawa M, et al. SRPX2 is overexpressed in gastric cancer and promotes cellular migration and adhesion. *Int J Cancer* 2009;124:1072–80.
22. United Kingdom Co-ordinating Committee on Cancer Research (UKCCCR). Guidelines for the Welfare of Animals in Experimental Neoplasia (Second Edition). *Br J Cancer* 1998;77:1–10.
23. Guix M, Faber AC, Wang SE, et al. Acquired resistance to EGFR tyrosine kinase inhibitors in cancer cells is mediated by loss of IGF-binding proteins. *J Clin Invest* 2008;118:2609–19.
24. Turke AB, Zejnullahu K, Wu YL, et al. Preexistence and clonal selection of MET amplification in EGFR mutant NSCLC. *Cancer Cell* 2010;17:77–88.
25. Tsao MS, Yang Y, Marcus A, Liu N, Mou L. Hepatocyte growth factor is predominantly expressed by the carcinoma cells in non-small-cell lung cancer. *Hum Pathol* 2001;32:57–65.
26. Ohitsuka T, Uramoto H, Nose N, et al. Acquired resistance to gefitinib: the contribution of mechanisms other than the T790M, MET, HGF status. *Lung Cancer* 2010;68:198–203.
27. Bhowmick NA, Neilson EG, Moses HL. Stromal fibroblasts in cancer initiation and progression. *Nature* 2004;432:332–7.
28. Matsumoto K, Nakamura T. Hepatocyte growth factor and the Met system as a mediator of tumor-stromal interactions. *Int J Cancer* 2006;119:477–83.
29. Wang W, Li Q, Yamada T, et al. Crosstalk to stromal fibroblasts induces resistance of lung cancer to epidermal growth factor receptor tyrosine kinase inhibitors. *Clin Cancer Res* 2009;15:6630–8.

Role of Survivin in EGFR Inhibitor–Induced Apoptosis in Non–Small Cell Lung Cancers Positive for *EGFR* Mutations

Kunio Okamoto¹, Isamu Okamoto¹, Wataru Okamoto¹, Kaoru Tanaka¹, Ken Takezawa¹, Kiyoko Kuwata¹, Haruka Yamaguchi¹, Kazuto Nishio², and Kazuhiko Nakagawa¹

Abstract

The molecular mechanism by which epidermal growth factor receptor–tyrosine kinase inhibitors (EGFR-TKI) induce apoptosis in non–small cell–lung cancer (NSCLC) cells that are positive for activating mutations of the EGFR remains unclear. In this study, we report the effects of the EGFR-TKI gefitinib on expression of the antiapoptotic protein survivin that have functional consequences in EGFR mutation–positive NSCLC cells. Immunoblot analysis revealed that gefitinib downregulated survivin expression, likely through inhibition of the PI3K–AKT signaling pathway, in NSCLC cells positive for EGFR mutation. Stable overexpression of survivin attenuated gefitinib-induced apoptosis and also inhibited the antitumor effect of gefitinib in human tumor xenografts. Furthermore, the combination of survivin overexpression with inhibition of the gefitinib-induced upregulation of the proapoptotic protein BIM attenuated gefitinib-induced apoptosis to a greater extent than either approach alone. Our results indicate that downregulation of survivin plays a pivotal role in gefitinib-induced apoptosis in EGFR mutation–positive NSCLC cells. Furthermore, they suggest that simultaneous interruption of the PI3K–AKT–survivin and MEK–ERK–BIM signaling pathways is responsible for EGFR-TKI–induced apoptotic death in these cells. *Cancer Res*; 70(24): 10402–10. © 2010 AACR.

Introduction

Survivin is a member of the inhibitor of apoptosis (IAP) family of proteins and has been shown to inhibit caspases and to prevent caspase-mediated cell death (1–3). Survivin is abundant in many types of cancer cells but not in the corresponding normal cells (4, 5). In nonmalignant proliferating cells, the expression of survivin is regulated in a cell cycle-dependent manner (6, 7). The upregulation of survivin expression in tumors does not seem to be dependent solely on the cell cycle, however, given that it occurs in tumor cells that are not actively cycling (4, 8, 9). Indeed, growth factors have been found to regulate survivin expression in endothelial cells and neuroblastoma cells (10, 11). Although expression of survivin has been demonstrated in non–small cell–lung cancer (NSCLC; refs. 12–14), the mechanism by which such expression is regulated in NSCLC cells has remained unknown.

The epidermal growth factor receptor (EGFR) is a receptor tyrosine kinase that is abnormally amplified or activated in a variety of tumors including NSCLC, and it has therefore been identified as an important target in cancer treatment (15–17). Inhibitors of the tyrosine kinase activity of EGFR (EGFR-TKI), which compete with ATP for binding to the tyrosine kinase pocket of the receptor, have been extensively studied in patients with NSCLC (18, 19). Several prospective clinical trials have revealed marked antitumor activity of EGFR-TKIs in NSCLC patients with *EGFR* mutations. The therapeutic benefit of these drugs is much greater than that historically observed with standard cytotoxic chemotherapy for advanced NSCLC. NSCLC cells with *EGFR* mutations manifest activation of the PI3K (phosphatidylinositol 3-kinase)–AKT and MEK–ERK (extracellular signal-regulated kinase) signaling pathways under the control of EGFR, and exposure of such cells to EGFR-TKIs blocks signaling by both pathways and induces apoptosis (20–22). The precise molecular mechanism by which EGFR-TKIs induce apoptosis has remained unclear, however. We have therefore now examined the effect of the EGFR-TKI gefitinib on survivin expression as well as further investigated the mechanism of gefitinib-induced apoptosis in *EGFR* mutation–positive NSCLC cells.

Authors' Affiliations: Departments of ¹Medical Oncology and ²Genome Biology, Kinki University School of Medicine, 377-2 Ohno-higashi, Osaka-Sayama, Osaka, Japan

Note: Supplementary data for this article are available at Cancer Research Online (<http://cancerres.aacrjournals.org/>).

Corresponding Author: Isamu Okamoto, Department of Medical Oncology, Kinki University School of Medicine, 377-2 Ohno-higashi, Osaka-Sayama, Osaka 589-8511, Japan. Phone: 81-72-366-0221; Fax: 81-72-366-5000; E-mail: chi-okamoto@doti.med.kindai.ac.jp

doi: 10.1158/0008-5472.CAN-10-2438

© 2010 American Association for Cancer Research.

Materials and Methods

Cell culture and reagents

The human NSCLC cell lines PC9, HCC827, NCI-H1975 (H1975), A549, and H1299 were obtained from American Type Culture Collection. The NSCLC line PC9/ZD was obtained as

described previously (23). All cells were cultured under a humidified atmosphere of 5% CO₂ at 37°C in RPMI 1640 medium (Sigma) supplemented with 10% fetal bovine serum. Gefitinib was obtained from Kemprotec, U0126 and LY294002 were from Cell Signaling Technology and BEZ235 and AZD6244 were from Shanghai Biochempartner.

Immunoblot analysis

Cells were washed twice with ice-cold PBS and then lysed in a solution containing 20 mmol/L Tris-HCl (pH 7.5), 150 mmol/L NaCl, 1 mmol/L EDTA, 1% Triton X-100, 2.5 mmol/L sodium pyrophosphate, 1 mmol/L phenylmethylsulfonyl fluoride, and leupeptin (1 µg/mL). The protein concentration of the cell lysates was determined with the use of the Bradford reagent (Bio-Rad), and equal amounts of protein were subjected to SDS-PAGE on a 7.5% gel. The separated proteins were transferred to a nitrocellulose membrane, which was then exposed to 5% nonfat dried milk in PBS for 1 hour at room temperature before incubation overnight at 4°C with primary antibodies. Rabbit polyclonal antibodies to human phosphorylated EGFR (pY1068), to XIAP, to phosphorylated and total AKT, to phosphorylated and total ERK, to poly(ADP-ribose) polymerase (PARP), to caspase-3, and to BIM were obtained from Cell Signaling Technology; those to survivin were from Santa Cruz Biotechnology; those to cIAP-1 were from R&D Systems; and those to β -actin were from Sigma. Mouse monoclonal antibodies to EGFR were obtained from Invitrogen. All antibodies were used at a 1:1,000 dilution, with the exception of those to β -actin (1:200). The nitrocellulose membrane was then washed with PBS containing 0.05% Tween 20 before incubation for 1 hour at room temperature with horseradish peroxidase-conjugated goat antibodies to rabbit (Sigma) or mouse (Santa Cruz Biotechnology) immunoglobulin G. Immune complexes were finally detected with chemiluminescence reagents (Perkin-Elmer Life Science).

Gene silencing

Cells were plated at 50% to 60% confluence in 6-well plates or 25-cm² flasks and then incubated for 24 hours before transient transfection for the indicated times with small interfering RNAs (siRNA) mixed with the Lipofectamine reagent (Invitrogen). The siRNAs specific for AKT (AKT-1, 5'-CAGGUUUUUUGAUGAGGA-3'; AKT-2, 5'-CAACCCGCAUCACAGACUGU-3'), survivin (survivin-1, 5'-GAAGCAGUUUGAAGAAUAU-3'; survivin-2, 5'-AGAAGCAGUUUGAAGAAUU-3'), or BIM (BIM-1, 5'-GGAGGGUUAUUUUUGAAUAU-3') mRNAs as well as corresponding scrambled (control) siRNAs were obtained from Nippon EGT.

Annexin V binding assay

The binding of Annexin V to cells was measured with the use of an Annexin-V-FLUOS Staining Kit (Roche). Cells were harvested by exposure to trypsin-EDTA, washed with PBS, and centrifuged at 200 × *g* for 5 minutes. The cell pellets were resuspended in 100 µL of Annexin-V-FLUOS labeling solution, incubated for 10 to 15 minutes at 15°C to 25°C, and then

analyzed for fluorescence with a flow cytometer (FACSCalibur) and Cell Quest software (Becton Dickinson).

Cell cycle analysis

Cells were harvested, washed with PBS, fixed with 70% methanol, washed again with PBS, and stained with propidium iodide (0.05 mg/mL) in a solution containing 0.1% Triton X-100, 0.1 mmol/L EDTA, and RNase A (0.05 mg/mL). The stained cells were then analyzed for DNA content with a flow cytometer and Modfit software (Verity Software House).

Establishment of cells stably overexpressing survivin

A full-length cDNA fragment encoding human survivin was obtained from HCC827 cells by reverse transcription and PCR with the primers survivin-forward (5'-GCGGCCGCGGGC-ATGGGTGCCCCGACGTG-3') and survivin-reverse (5'-GGATCCTCAATCCATGGCAGCCAGCTGCTCG-3'). The amplification product was verified by sequencing after its cloning into the pCR-Blunt II-TOPO vector (Invitrogen). The survivin cDNA was excised from pCR-Blunt II-TOPO and transferred to the pQCXIH retroviral vector (Clontech). Retroviruses encoding survivin were then produced and used to infect PC9 and HCC827 cells as described (24). Cells stably expressing survivin were then isolated by selection with hygromycin at 300 µg/mL (Invivogen).

Growth inhibition assay *in vivo*

All animal studies were performed in accordance with the Recommendations for Handling of Laboratory Animals for Biomedical Research compiled by the Committee on Safety and Ethical Handling Regulations for Laboratory Animal Experiments, Kinki University (Osaka, Japan). The ethical procedures followed conformed to the guidelines of the United Kingdom Coordinating Committee on Cancer Prevention Research. Tumors cells (5 × 10⁶) were injected subcutaneously into the axilla of 5- to 6-week-old female athymic nude mice (BALB/c nu/nu; CLEA Japan). Treatment was initiated when tumors in each group of 6 mice achieved an average volume of 200 to 400 mm³. Treatment groups consisted of vehicle control and gefitinib (10 or 25 mg/kg). Gefitinib was administered by oral gavage daily for 4 weeks, with control animals receiving a 0.5% (w/v) aqueous solution of hydroxypropylmethylcellulose as vehicle. Tumor volume was determined from caliper measurements of tumor length (*L*) and width (*W*) according to the formula $LW^2/2$. Both tumor size and body weight were measured twice per week.

Statistical analysis

Quantitative data are presented as means ± SE from 3 independent experiments or for 6 animals per group unless indicated otherwise. The significance of differences in the percentage of Annexin V-positive cells was evaluated with the unpaired 2-tailed Student's *t* test. *P* < 0.05 was considered statistically significant.

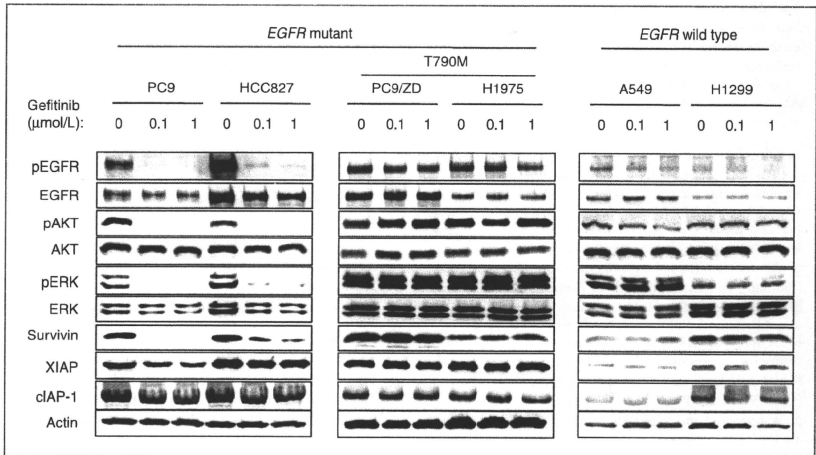


Figure 1. Effects of gefitinib on the expression of IAP family proteins in human NSCLC cells. PC9, HCC827, PC9/ZD, H1975, A549, or H1299 cells were incubated in complete medium and in the presence of the indicated concentrations of gefitinib for 24 hours. Cell lysates were then prepared and subjected to immunoblot analysis with antibodies to phosphorylated (p) or total forms of EGFR, AKT, or ERK, to survivin, to XIAP, to cIAP-1, or to β -actin (loading control). Data are representative of 3 independent experiments.

Results

Gefitinib downregulates survivin expression in EGFR mutation-positive NSCLC cell lines

We first examined the effects of the EGFR-TKI gefitinib on the expression of IAP family members in a subset of NSCLC cell lines (PC9, HCC827, PC9/ZD, H1975, A549, and H1299) by immunoblot analysis (Fig. 1). PC9 and HCC827 cells harbor an EGFR allele with an activating mutation, whereas A549 and H1299 cells express wild-type EGFR and PC9/ZD and H1975 cells harbor an EGFR allele with both an activating mutation and a mutation (T790M) that confers resistance to EGFR-TKIs. In PC9 and HCC827 cells, gefitinib induced the dephosphorylation of EGFR and reduced the abundance of survivin in a concentration-dependent manner. In contrast, in cells expressing wild-type EGFR or harboring the T790M resistance mutation, gefitinib did not affect the phosphorylation level of EGFR or the expression of survivin. The expression of other IAP family members, including XIAP and cIAP-1, was not substantially affected by gefitinib in any of the cell lines examined. These data thus showed that gefitinib downregulated survivin expression in NSCLC cells with an activating mutation of EGFR.

Inhibition of the PI3K-AKT pathway results in survivin downregulation in EGFR mutation-positive cells

To identify the signaling pathway (or pathways) responsible for downregulation of survivin by gefitinib, we exam-

ined the effects of specific inhibitors of MEK (U0126 and AZD6244) and PI3K (LY294002 and BEZ235) in EGFR mutation-positive NSCLC cells (PC9 and HCC827). Each of the PI3K inhibitors reduced the abundance of survivin, whereas the MEK inhibitors had no such effect (Fig. 2A), suggesting that the regulation of survivin expression is mediated by PI3K rather than by MEK in EGFR mutation-positive NSCLC cells. Given that the protein kinase AKT is an important downstream target of PI3K, we examined whether the PI3K-dependent survivin expression is also dependent on AKT. Depletion of AKT by transfection of cells with 2 different siRNAs specific for AKT mRNA (AKT-1 and AKT-2 siRNA) resulted in downregulation of survivin expression in both PC9 and HCC827 cells (Fig. 2B). These results thus suggested that gefitinib might regulate survivin expression through inhibition of the PI3K-AKT signaling pathway in EGFR mutation-positive NSCLC cells.

Knockdown of survivin expression induces apoptosis in EGFR mutation-positive cells

To investigate whether downregulation of survivin by gefitinib is related to gefitinib-induced apoptosis, we transfected PC9 or HCC827 cells with 2 independent siRNA specific for survivin mRNA (survivin-1 and survivin-2 siRNAs). Depletion of survivin resulted in generation of the cleaved forms of both caspase-3 and PARP in both cell lines (Fig. 3A). Staining with Annexin V also revealed that the proportion of apoptotic cells was markedly increased by transfection with the survivin

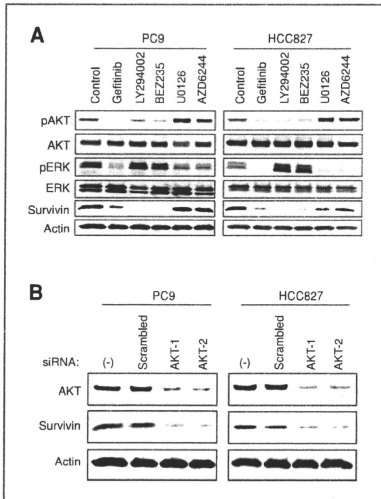


Figure 2. Effects of inhibition of MEK or PI3K signaling pathways on survivin expression in EGFR mutation-positive NSCLC cells. A, PC9 or HCC827 cells were incubated in the absence (control, 0.1% dimethyl sulfoxide) or the presence of gefitinib (1 $\mu\text{mol/L}$), LY294002 (20 $\mu\text{mol/L}$), BEZ235 (0.2 $\mu\text{mol/L}$), U0126 (20 $\mu\text{mol/L}$), or AZD6244 (0.2 $\mu\text{mol/L}$) for 24 hours, after which cell lysates were prepared and subjected to immunoblot analysis with antibodies to phosphorylated (p) or total forms of AKT or ERK, to survivin, or to β -actin. B, Cells were transfected (or not) with 2 different AKT (AKT-1 or AKT-2) or scrambled (control) siRNAs for 48 hours, lysed, and subjected to immunoblot analysis with antibodies to AKT, to survivin, or to β -actin. All data are representative of 3 independent experiments.

siRNAs (Fig. 3B). In addition, depletion of survivin resulted in an increase in the size of the sub- G_1 (apoptotic) cell population, as revealed by flow cytometry (Fig. 3C). These data suggested that downregulation of survivin induces apoptosis in EGFR mutation-positive NSCLC cells.

Overexpression of survivin inhibits gefitinib-induced apoptosis in EGFR mutation-positive cells *in vitro*

To examine further the role of survivin in gefitinib-induced apoptosis, we established PC9 and HCC827 sublines (PC9S7, PC9S8, HCC827S6, and HCC827S7) that stably overexpress survivin as a result of retroviral infection. The abundance of survivin in these sublines was substantially greater than that in cells infected with the empty virus (PC9-Mock and HCC827-Mock; Fig. 4A). In addition, gefitinib markedly reduced the level of survivin expression in PC9-Mock and HCC827-Mock cells but not in the corresponding sublines overexpressing survivin (Fig. 4B). Immunoblot ana-

lysis of the cleaved forms of caspase-3 and PARP (Fig. 4B) as well as staining with Annexin V (Fig. 4C) also revealed that overexpression of survivin resulted in marked inhibition of gefitinib-induced apoptosis. Examination of the effect of gefitinib on cell cycle distribution revealed that gefitinib increased the proportion of cells in G_0 - G_1 phase and reduced that in S phase at 24 hours in a manner independent of survivin overexpression (Fig. 4D). The survivin-overexpressing sublines, however, showed a smaller time-dependent increase in the size of the sub- G_1 cell population than did cells infected with the empty virus. These results thus further indicated that downregulation of survivin by gefitinib contributes to the proapoptotic action of this drug in EGFR mutation-positive NSCLC cells.

Overexpression of survivin inhibits the antitumor effect of gefitinib on EGFR mutation-positive cells *in vivo*

To investigate whether the antitumor effect of gefitinib on EGFR mutation-positive NSCLC cells might be affected by survivin overexpression *in vivo*, we injected HCC827-Mock cells or cells of the survivin-overexpressing subline HCC827S7 into nude mice for elicitation of the formation of solid tumors. When the tumors became palpable (200–400 mm^3), mice were divided into 3 groups and treated with vehicle (control) or gefitinib at a daily dose of 10 or 25 mg/kg by oral gavage for 4 weeks. Gefitinib treatment at either dose eradicated tumors in mice injected with HCC827-Mock cells (Fig. 5A and C). In contrast, tumors in mice injected with survivin-overexpressing cells were not eradicated by gefitinib even at the dose of 25 mg/kg per day, although tumor growth was partially inhibited by gefitinib in a dose-dependent manner (Fig. 5B and C). These results showed that survivin overexpression inhibits the antitumor effect of gefitinib on EGFR mutation-positive NSCLC cells *in vivo*.

Effect of attenuation of BIM induction on gefitinib-induced apoptosis in EGFR mutation-positive cells overexpressing survivin

Survivin overexpression did not completely eliminate gefitinib-induced apoptosis in PC9 and HCC827 cells, suggesting that other signaling pathways might contribute to this process. Induction of the proapoptotic BH3-only protein BIM has been found to be important for EGFR-TKI-induced apoptosis in EGFR mutation-positive lung cancers, and inhibition of the EGFR-MEK-ERK signaling pathway is required for BIM induction (25–27). We therefore examined whether survivin overexpression in combination with specific inhibition of BIM induction results in an additive antiapoptotic effect in EGFR mutation-positive NSCLC cells. We transiently transfected survivin-overexpressing sublines of PC9 or HCC827 cells with an siRNA specific for BIM mRNA. Transfection with the BIM siRNA specifically inhibited the induction of BIM expression by gefitinib in both mock-infected and survivin-overexpressing sublines (Fig. 6A). Staining with Annexin V further revealed that the combination of survivin overexpression and attenuation of BIM induction resulted in a greater level of inhibition of gefitinib-induced apoptosis than that observed with either approach alone (Fig. 6B). These data were

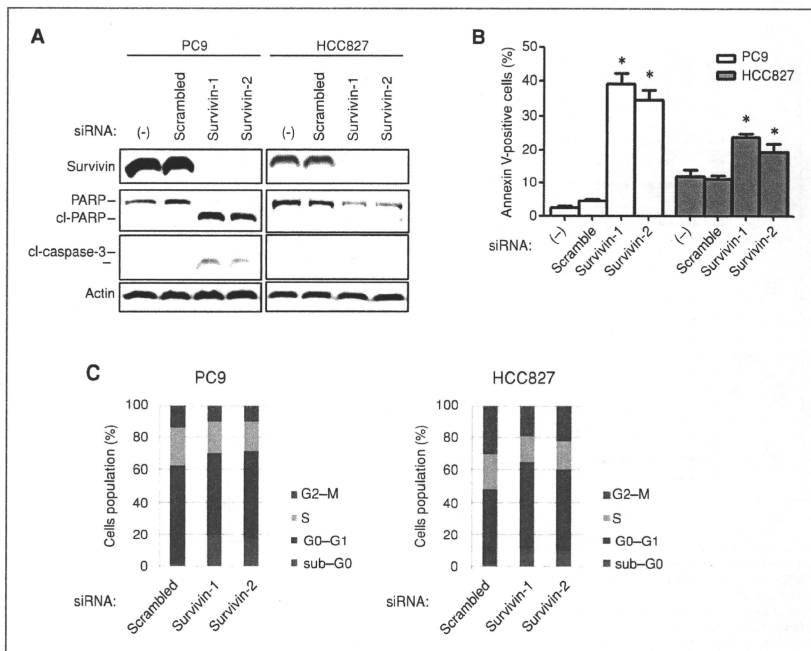


Figure 3. Effect of survivin depletion on apoptosis in *EGFR* mutation-positive NSCLC cells. **A**, PC9 or HCC827 cells were transfected (or not) with 2 different survivin (survivin-1 or survivin-2) or scrambled (control) siRNAs for 48 hours, after which cell lysates were prepared and subjected to immunoblot analysis with antibodies to survivin, to PARP, to caspase-3, or to β -actin. Bands corresponding to the cleaved (cl) forms of caspase-3 and PARP are indicated. Data are representative of 3 independent experiments. **B**, cells were transfected with survivin or scrambled siRNAs for 72 hours, after which the proportion of apoptotic cells was determined by staining with fluorescein isothiocyanate-conjugated Annexin V and propidium iodide followed by flow cytometry. Data are means \pm SE from 3 independent experiments. *, $P < 0.05$ versus the corresponding value for cells transfected with the scrambled siRNA. **C**, cells were transfected with survivin or scrambled siRNAs for 48 hours, fixed, stained with propidium iodide, and analyzed for cell cycle distribution by flow cytometry. Data are means of triplicates from representative experiments that were repeated 3 times.

confirmed with a second BIM siRNA to rule out off-target effects (Supplementary Fig. 1). These results thus suggested that both survivin downregulation and BIM induction contribute independently to gefitinib-induced apoptosis in *EGFR* mutation-positive NSCLC cells.

Discussion

EGFR-TKIs induce marked clinical responses in patients with NSCLC positive for activating mutations of *EGFR* (1-3). *In vitro* experiments have shown that EGFR-TKIs induce a substantial level of apoptosis in NSCLC cell lines expressing mutant EGFRs (4). However, the key downstream mediators

of EGFR-TKI-induced apoptosis in *EGFR* mutation-positive cells have remained unidentified. We have now found that gefitinib downregulated survivin expression in *EGFR* mutation-positive NSCLC cells but not in NSCLC cells expressing wild-type EGFR or EGFR with the T790M resistance mutation. With the use of specific PI3K inhibitors and siRNAs specific for AKT mRNA, we further showed that the downregulation of survivin expression by gefitinib is likely mediated through inhibition of PI3K-AKT signaling. Human epidermal growth factor receptor 2 (*HER2*)-targeting agents such as lapatinib and trastuzumab were previously found to induce downregulation of survivin through inhibition of the PI3K-AKT pathway in breast cancer cells positive for *HER2* amplification

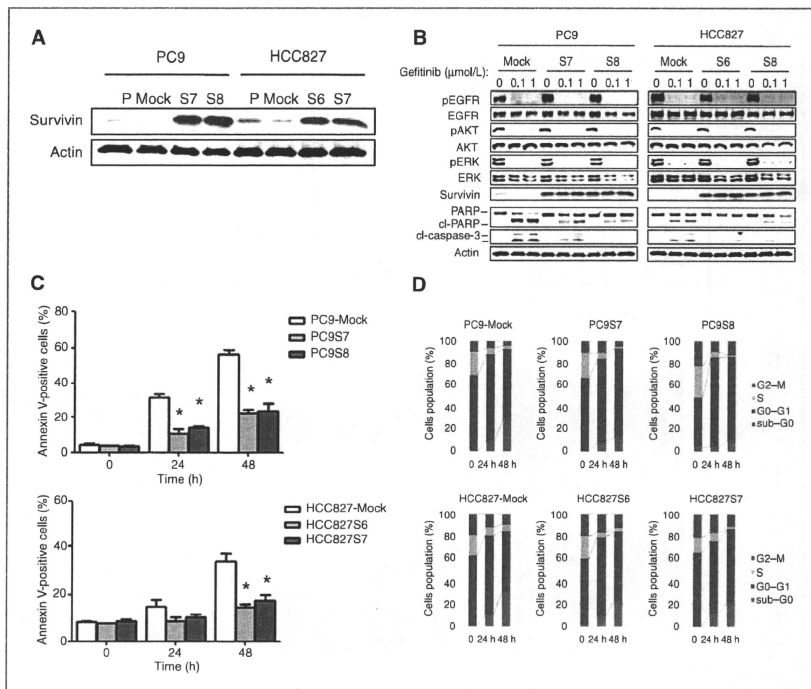


Figure 4. Effect of survivin overexpression on gefitinib-induced apoptosis in EGFR mutation-positive NSCLC cells *in vitro*. **A**, parental (P) PC9 or HCC827 cells or corresponding sublines either stably overexpressing survivin (PC9S7, PC9S8, HCC827S6, and HCC827S7) or infected with the empty retrovirus (PC9-Mock and HCC827-Mock) were cultured overnight in complete medium, after which cell lysates were prepared and subjected to immunoblot analysis with antibodies to survivin or to β -actin. **B**, PC9 or HCC827 isogenic cell lines were incubated in the presence of the indicated concentrations of gefitinib for 48 hours, after which cell lysates were prepared and subjected to immunoblot analysis with antibodies to phosphorylated (p) or total forms of EGFR, AKT, or ERK, to survivin, to PARP, to caspase-3, or to β -actin. Data in **A** and **B** are representative of 3 independent experiments. **C**, PC9 or HCC827 isogenic cell lines were incubated with gefitinib (0.1 μ mol/L) for the indicated times, after which the proportion of apoptotic cells was determined by staining with Annexin V and propidium iodide followed by flow cytometry. Data are means \pm SE from 3 independent experiments. *, $P < 0.05$ versus the corresponding value for cells infected with the empty retrovirus. **D**, PC9 or HCC827 isogenic cell lines were incubated with gefitinib (0.1 μ mol/L) for the indicated times and then analyzed for cell cycle distribution by flow cytometry. Data are means of triplicates from representative experiments that were repeated 3 times.

(28, 29). Given that downregulation of survivin through inhibition of the PI3K-AKT pathway was induced by EGFR-TKIs in EGFR mutation-positive NSCLC cells and by HER2-targeting agents in breast cancer cells positive for HER2 amplification, the expression of survivin is likely dependent on PI3K-AKT signaling that operates downstream of receptor tyrosine kinases and is essential for cell survival. This hypothesis is further supported by the observation that transfection of EGFR mutation-positive NSCLC cells with an siRNA specific

for EGFR mRNA resulted in marked inhibition of survivin expression, whereas transfection of cells expressing wild-type EGFR had no such effect (Supplementary Fig. 2). The PI3K-AKT pathway has been implicated in the regulation of survivin expression by cytokines, growth factors, and chemotherapeutic drugs (8, 10, 30). Although no direct correlation has been established between downregulation of survivin and inhibition of EGFR signaling, these previous findings support the notion that inhibition of the EGFR-PI3K-AKT pathway

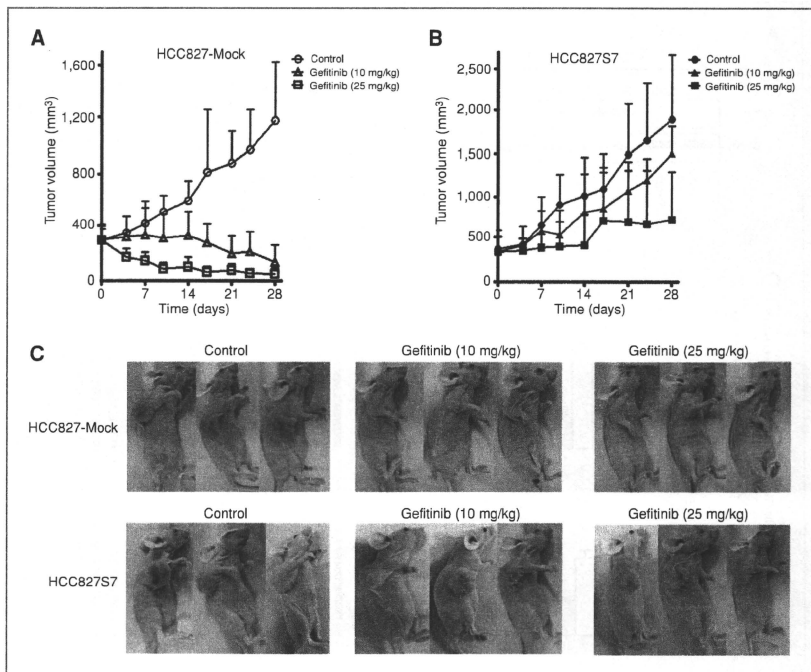


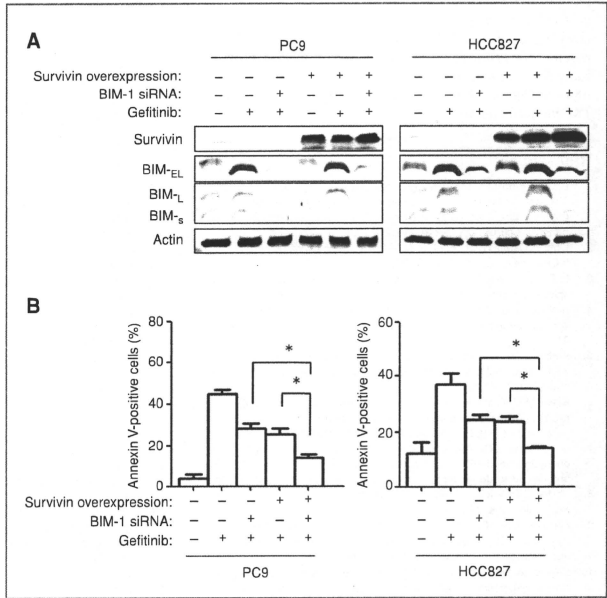
Figure 5. Effect of gefitinib on the growth of EGFR mutation-positive NSCLC cells overexpressing survivin in vivo. A and B, nude mice with tumor xenografts established by subcutaneous injection of HCC827-Mock or HCC827S7 cells, respectively, were treated daily for 4 weeks with vehicle (control) or gefitinib (10 or 25 mg/kg). Tumor volume was determined at the indicated times after the onset of treatment. Data are means \pm SE of values from 6 mice per group. C, representative mice showing tumors at the end of the 4-week treatment period.

contributes to downregulation of survivin expression by EGFR-TKIs in *EGFR* mutation-positive NSCLC cells.

Survivin has been implicated in resistance of cancer cells to apoptosis, although the effect of survivin expression on gefitinib-induced apoptosis in *EGFR* mutation-positive NSCLC cells has not previously been examined. We have now shown that survivin overexpression inhibited gefitinib-induced apoptosis in such cells. Inhibition of the PI3K-AKT and MEK-ERK pathways was previously found to account for much of the proapoptotic activity of EGFR-TKIs in *EGFR* mutation-positive NSCLC cells (31). We further found that overexpression of survivin resulted in inhibition of apoptosis induced by a combination of PI3K and MEK inhibitors in such cells (Supplementary Fig. 3). Increased AKT activity as a result either of the loss of PTEN or of expression of a constitutively active

form of AKT was previously found to be associated with a reduced sensitivity to EGFR-TKIs in *EGFR* mutation-positive NSCLC cells (32). However, the principal molecular target underlying the response to inhibition of PI3K-AKT signaling by EGFR-TKIs has remained to be elucidated. In the present study, we show that the sensitivity of *EGFR* mutation-positive NSCLC cells to EGFR-TKIs depends, at least in part, on survivin downregulation through inhibition of the PI3K-AKT pathway. In our xenograft model, we showed that survivin overexpression inhibited the antitumor effect of gefitinib on *EGFR* mutation-positive NSCLC cells. The extent of the clinical benefit of EGFR-TKIs varies among NSCLC patients harboring activating *EGFR* mutations, and the efficacy of these drugs is limited by either *de novo* resistance or resistance acquired after the onset of therapy (33). Although several

Figure 6. Effect of the combination of survivin overexpression and inhibition of BIM induction on gefitinib-induced apoptosis in *EGFR* mutation-positive NSCLC cells. **A**, cells stably overexpressing survivin (PC9S7 and HCC827S6) or infected with the empty retrovirus (PC9-Mock and HCC827-Mock) were transfected with BIM₁ (BIM-1) or scrambled siRNAs for 24 hours and then incubated for 24 hours in complete medium with or without gefitinib (0.1 μ M/L). Cell lysates were then prepared and subjected to immunoblot analysis with antibodies to survivin, to BIM, or to β -actin. Data are representative of 3 independent experiments. **B**, cells transfected as in (A) were incubated for 48 hours in the absence or presence of gefitinib (0.1 μ M/L) and then evaluated for the proportion of apoptotic cells by staining with Annexin V and propidium iodide followed by flow cytometry. Data are means \pm SE from 3 independent experiments. *, $P < 0.05$ for the indicated comparisons.



mechanisms of acquired resistance have been described, it remains of clinical concern that molecular markers for prediction of *de novo* resistance to these drugs have not been well delineated (23, 34–38). It will therefore be of interest to determine whether increased survivin expression in tumors is clinically useful as a negative predictive marker of sensitivity to EGFR-TKIs in patients with *EGFR* mutation-positive NSCLC.

Our observations revealed that survivin overexpression did not completely abolish gefitinib-induced apoptosis, suggesting that another proapoptotic regulator activated after EGFR inhibition might contribute to EGFR-TKI-induced apoptotic cell death. Previous studies have shown that gefitinib induces BIM expression via inhibition of the MEK-ERK pathway and that BIM induction plays a key role in EGFR-TKI-induced apoptosis in *EGFR* mutation-positive NSCLC cells (25–27). We have now shown that inhibition of both survivin downregulation and BIM induction attenuated gefitinib-induced apoptosis to a greater extent than did inhibition of either process alone. The recent preclinical study showing that the combination of a PI3K inhibitor and a MEK inhibitor, but neither agent alone, induced substantial growth inhibition in *EGFR* mutation-positive NSCLC cells (31) supports the notion that both the PI3K-AKT-survivin and MEK-ERK-BIM pathways contri-

bute independently to gefitinib-induced apoptosis in such cells (Fig. 7).

In conclusion, we have shown that the EGFR-TKI gefitinib downregulated survivin expression, likely through inhibition

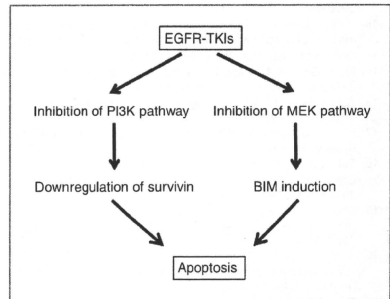


Figure 7. Proposed model for the intracellular signaling underlying EGFR-TKI-induced apoptosis in *EGFR* mutation-positive NSCLC cells.

of PI3K-AKT signaling, and that this effect plays a key role in gefitinib-induced apoptosis. Moreover, we found that survivin downregulation and BIM induction are independently required for EGFR-TKI-induced apoptosis. Our results thus show that simultaneous upstream interruption of the PI3K-AKT-survivin and MEK-ERK-BIM pathways mediates EGFR-TKI-induced apoptosis.

Disclosure of Potential Conflicts of Interest

No potential conflicts of interest were disclosed.
The costs of publication of this article were defrayed in part by the payment of page charges. This article must therefore be hereby marked *advertisement* in accordance with 18 U.S.C. Section 1734 solely to indicate this fact.

Received 07/06/2010; revised 09/11/2010; accepted 10/08/2010; published Online 12/15/2010.

References

- Blanco-Bruide OP, Mesri M, Wall NR, Plecia J, Dohi T, Altieri DC. Therapeutic targeting of the survivin pathway in cancer: initiation of mitochondrial apoptosis and suppression of tumor-associated angiogenesis. *Clin Cancer Res* 2003;9:2683-92.
- Dohi T, Okada K, Xia F, et al. An IAP-IAP complex inhibits apoptosis. *J Biol Chem* 2004;279:34087-90.
- Li F, Ambrosini G, Chu EY, et al. Control of apoptosis and mitotic spindle checkpoint by survivin. *Nature* 1998;396:580-4.
- Ambrosini G, Adida C, Altieri DC. A novel anti-apoptosis gene, survivin, expressed in cancer and lymphoma. *Nat Med* 1997;3:917-21.
- Ambrosini G, Adida C, Sirugo G, Altieri DC. Induction of apoptosis and inhibition of cell proliferation by survivin gene targeting. *J Biol Chem* 1998;273:11177-82.
- Kallio MJ, Nieminen M, Eriksson JE. Human inhibitor of apoptosis protein (IAP) survivin participates in regulation of chromosome segregation and mitotic exit. *FASEB J* 2001;15:2721-3.
- Li F, Altieri DC. The cancer antiapoptosis mouse survivin gene: characterization of locus and transcriptional requirements of basal and cell cycle-dependent expression. *Cancer Res* 1999;59:3143-51.
- Carter BZ, Milella M, Altieri DC, Andreoff M. Cytokine-regulated expression of survivin in myeloid leukemia. *Blood* 2001;97:2784-90.
- Fang ZH, Dong CL, Chen Z, et al. Transcriptional regulation of survivin by c-Myc in BCR/ABL-transformed cells: implications in anti-leukemic strategy. *J Cell Mol Med* 2009;13:2039-52.
- Beierle EA, Nagaram A, Dai W, Yengar M, Chen MK. VEGF-mediated survivin expression in neuroblastoma cells. *J Surg Res* 2005;127:21-8.
- Tran J, Master Z, Yu JL, Rak J, Dumont DJ, Kerbel RS. A role for survivin in chemoresistance of endothelial cells mediated by VEGF. *Proc Natl Acad Sci U S A* 2002;99:4349-54.
- Fan J, Wang L, Jiang GN, He WX, Ding JA. The role of survivin on overall survival of non-small cell lung cancer: a meta-analysis of published literatures. *Lung Cancer* 2008;61:91-6.
- Huang CL, Liu D, Nakano J, et al. E2F1 overexpression correlates with thymidylate synthase and survivin gene expressions and tumor proliferation in non-small-cell lung cancer. *Clin Cancer Res* 2007;13:6938-46.
- Krepela E, Dankova P, Moravcikova E, et al. Increased expression of inhibitor of apoptosis proteins, survivin and XIAP, in non-small cell lung carcinoma. *Int J Oncol* 2009;35:1449-62.
- Mendelsohn J, Baselga J. The EGFR receptor family as targets for cancer therapy. *Oncogene* 2000;19:6550-65.
- Schlessinger J. Cell signaling by receptor tyrosine kinases. *Cell* 2000;103:211-25.
- Hynes NE, Lane HA. ERBB receptors and cancer: the complexity of targeted inhibitors. *Nat Rev Cancer* 2005;5:341-54.
- Paez JG, Janne PA, Lee JC, et al. EGFR mutations in lung cancer: correlation with clinical response to gefitinib therapy. *Science* 2004;304:1497-500.
- Shepherd FA, Rodrigues Pereira J, Ciuleanu T, et al. Erlotinib in previously treated non-small-cell lung cancer. *N Engl J Med* 2005;353:123-32.
- Sordella R, Bell DW, Haber DA, Getteman J. Gefitinib-sensitizing EGFR mutations in lung cancer activate anti-apoptotic pathways. *Science* 2004;305:1163-7.
- Tracy S, Mukohara T, Hansen M, Meyerson M, Johnson BE, Janne PA. Gefitinib induces apoptosis in the EGFRL858R non-small-cell lung cancer cell line H3255. *Cancer Res* 2004;64:7241-4.
- Ling YH, Lin R, Perez-Soler R. Erlotinib induces mitochondrial-mediated apoptosis in human H3255 non-small-cell lung cancer cells with epidermal growth factor receptorL858R mutation through mitochondrial oxidative phosphorylation-dependent activation of BAX and BAK. *Mol Pharmacol* 2008;74:793-806.
- Kozumi F, Shimoyama T, Taguchi F, Saji N, Nishio K. Establishment of a human non-small cell lung cancer cell line resistant to gefitinib. *Int J Cancer* 2005;116:36-44.
- Tanaka K, Arai T, Maegawa M, et al. SFRP2 is overexpressed in gastric cancer and promotes cellular migration and adhesion. *Int J Cancer* 2009;124:1072-80.
- Costa DB, Halmos B, Kumar A, et al. BIM mediates EGFR tyrosine kinase inhibitor-induced apoptosis in lung cancers with oncogenic EGFR mutations. *PLoS Med* 2007;4:1669-79; discussion 80.
- Cragg MS, Kuroda J, Puthalath KK, Huang DC, Strasser A. Gefitinib-induced killing of NSCLC cell lines expressing mutant EGFR requires BIM and can be enhanced by BH3 mimetics. *PLoS Med* 2007;4:1681-89; discussion 90.
- Gong Y, Somwar R, Politi K, et al. Induction of BIM is essential for apoptosis triggered by EGFR kinase inhibitors in mutant EGFR-dependent lung adenocarcinomas. *PLoS Med* 2007;4:1655-68.
- Asanuma H, Torjoto T, Kamiguchi K, et al. Survivin expression is regulated by coexpression of human epidermal growth factor receptor 2 and epidermal growth factor receptor via phosphatidylinositol 3-kinase/AKT signaling pathway in breast cancer cells. *Cancer Res* 2005;65:11019-25.
- Xia W, Bisi J, Strum J, et al. Regulation of survivin by ErbB2 signaling: therapeutic implications for ErbB2-overexpressing breast cancers. *Cancer Res* 2008;68:1640-7.
- Zhao P, Meng Q, Liu LZ, You YP, Liu N, Jiang BH. Regulation of survivin by PI3K/Akt/p70S6K1 pathway. *Biochem Biophys Res Commun* 2010;395:219-24.
- Faber AC, Li D, Song Y, et al. Differential induction of apoptosis in HER2 and EGFR addicted cancers following PI3K inhibition. *Proc Natl Acad Sci U S A* 2009;106:19503-8.
- Sos ML, Koker M, Weir BA, et al. PTEN loss contributes to erlotinib resistance in EGFR-mutant lung cancer by activation of Akt and EGFR. *Cancer Res* 2009;69:3256-61.
- Okamoto I. Epidermal growth factor receptor in tumor development: EGFR-targeted anticancer therapy. *FEBS J* 2009;277:309-15.
- Engelman JA, Zejnullahu K, Mitsudomi T, et al. MET amplification leads to gefitinib resistance in lung cancer by activating ERBB3 signaling. *Science* 2007;316:1039-43.
- Ercan D, Zejnullahu K, Yonesaka K, et al. Amplification of EGFR T790M causes resistance to an irreversible EGFR inhibitor. *Oncogene* 2010;29:2346-56.
- Fao W, Miller VA, Politi KA, et al. Acquired resistance of lung adenocarcinomas to gefitinib or erlotinib is associated with a second mutation in the EGFR kinase domain. *PLoS Med* 2005;2:225-35.
- Yano S, Wang W, Li Q, et al. Hepatocyte growth factor induces gefitinib resistance of lung adenocarcinoma with epidermal growth factor receptor-activating mutations. *Cancer Res* 2008;68:9479-87.
- Takeda M, Okamoto I, Fujita Y, et al. *De novo* resistance to epidermal growth factor receptor-tyrosine kinase inhibitors in EGFR mutant positive patients with non-small cell lung cancer. *J Thorac Oncol* 2010;5:399-400.

Phase I Clinical and Pharmacokinetic Study of RAD001 (Everolimus) Administered Daily to Japanese Patients with Advanced Solid Tumors

Isamu Okamoto¹, Toshihiko Doi², Atsushi Ohtsu², Masaki Miyazaki¹, Asuka Tsuya³, Katsutoshi Kurei⁴, Ken Kobayashi⁴ and Kazuhiko Nakagawa¹

¹Department of Medical Oncology, Kinki University School of Medicine, Osaka, ²Division of Gastrointestinal Oncology/Digestive Endoscopy, National Cancer Center Hospital East, Chiba, ³Division of Thoracic Oncology, Shizuoka Cancer Center, Shizuoka and ⁴Novartis Pharma K.K., Tokyo, Japan

For reprints and all correspondence: Isamu Okamoto, Department of Medical Oncology, Kinki University School of Medicine, 377-2 Ohno-higashi, Osaka-Sayama, Osaka 589-8511, Japan. E-mail: chi-okamoto@dotd.med.kindai.ac.jp

Received July 8, 2009; accepted August 14, 2009

Objective: To determine the pharmacokinetics and safety of RAD001 (everolimus) in Japanese patients with advanced solid tumors.

Methods: An open-label, non-randomized, dose-escalation Phase I study of RAD001 administered continuously once daily in a 28-day cycle was performed. The study had a '3 + 3' design, with three patients recruited to each of three successive cohorts treated with RAD001 at 2.5, 5.0 or 10.0 mg/day.

Results: The pharmacokinetics of RAD001 in Japanese patients were similar to those previously determined in Caucasians. The drug safety profile was consistent with that of a mammalian target of rapamycin inhibitor. No dose-limiting toxicities were observed. One patient with esophageal cancer and one with gastric cancer treated with RAD001 at 10 mg/day showed marked tumor responses.

Conclusions: Treatment of Japanese cancer patients with RAD001 may be undertaken with the expectation that previously determined pharmacokinetic and safety profiles apply. The drug may hold promise for treatment of esophageal and gastric cancer.

Key words: Phase I study – pharmacokinetics – mTOR – RAD001 – everolimus

INTRODUCTION

Mammalian target of rapamycin (mTOR) is an intracellular protein kinase that mediates cellular responses to growth factors, nutrients and changes in energy status and thereby plays an important role in the regulation of cell growth, cell division and angiogenesis. It controls ribosome biosynthesis and the transcription of genes for many proteins that participate in the cell cycle, metabolism, nutrient transport or utilization, or the response to hypoxia. Various signaling defects upstream of mTOR, some of which are relatively common, have been identified in cancer cells and result in loss of cell growth control, unrestrained proliferation, tumor

angiogenesis, and other malignant characteristics. Defects in mTOR itself have not been identified in cancer, rendering this kinase both a well-situated and stable target for therapeutic intervention in cancers driven by defects in the mTOR signaling pathway (1–3).

RAD001 (everolimus) blocks the mTOR pathway by forming a complex with the immunophilin FK506-binding protein-12, which also binds mTOR with high affinity. This drug has exhibited antitumor activity with a variety of cancer cells both *in vitro* (4–9) and *in vivo* (10–12). In addition, the anticancer effects of RAD001 complement those of chemotherapy, radiation, hormonal agents and targeted therapeutics (13–15). RAD001 inhibits tumor growth

dependent on angiogenesis by inhibiting the production of angiogenic growth factors and thereby reducing the proliferation of neovascular endothelial cells (3). Phase I studies of RAD001 have shown sustained inhibition of mTOR activity in tumor tissue at oral doses of ≥ 20 mg weekly or 5–10 mg daily (16). Continuous daily dosing with RAD001 has been found to result in a more profound and sustained inhibition of mTOR than that achieved with an intermittent weekly schedule (17,18).

We have now performed a Phase I trial of RAD001 administered daily to Japanese patients with advanced solid tumors. The purpose of our study was to assess the pharmacokinetics, safety and tolerability of escalating oral doses of RAD001 in this patient population. An additional objective included evaluation of antitumor activity.

We herein report that RAD001 can be safely administered at daily doses up to 10 mg to Japanese patients with advanced solid malignancies. A dosage of 10 mg/day is recommended for further development.

PATIENTS AND METHODS

PATIENT POPULATION

Japanese individuals ≥ 20 years of age with a histologically confirmed diagnosis of an advanced tumor refractory to or unsuitable for existing standard therapy were included in the study if they had > 1 measurable lesion, a life expectancy of ≥ 3 months, and adequate or acceptable renal [serum creatinine concentration of $\leq 1.5 \times$ the upper limit of normal (ULN)], liver (serum bilirubin concentration of $\leq 1.25 \times$ ULN, serum transaminase activity of $\leq 3 \times$ ULN and serum albumin concentration of ≥ 3.5 g/dl) and bone marrow (absolute neutrophil count of $\geq 1500/\text{mm}^3$, platelet count of $\geq 1 \times 10^5/\text{mm}^3$ and hemoglobin concentration of ≥ 9 g/dl) function. Patients with tumors or metastases in the central nervous system, uncontrolled infection, gastrointestinal impairment disease, active bleeding diathesis, other concurrent or uncontrolled medical disease, or a history of coagulation disorders as well as those under treatment with strong inhibitors or inducers of isoenzyme CYP3A4 were excluded from the study. All subjects provided written informed consent to participation in the study, which was approved by the Institutional Review Board of each participating center and was performed in accordance with the Declaration of Helsinki and Good Clinical Practice guidelines.

STUDY DESIGN

The study was an open-label, non-randomized, dose-escalation Phase I trial of RAD001 administered on a continuous once-daily schedule in a 28-day cycle to adult Japanese patients, with continuation of therapy after 28 days in the absence of progressive disease. The primary objective was to evaluate the tolerability/safety and dose-limiting toxicity (DLT) of RAD001, up to the dose level of 10 mg/day

which is being used in the global study. The study had a '3 + 3' design, with three patients recruited to each of three successive cohorts treated with RAD001 at 2.5, 5.0 or 10.0 mg/day. Patients were allowed to receive a higher RAD001 dose, at the investigator's discretion, if the higher dose had been confirmed as tolerable. Treatment was discontinued in the event of progressive disease, DLT, a dose delay of > 14 days (or > 42 days for hematologic DLTs), or withdrawal of consent. A DLT was defined as a hematologic (anemia, leukopenia, thrombocytopenia or neutropenia) or non-hematologic adverse event with a grade of ≥ 3 or a laboratory abnormality with a grade of ≥ 3 that occurred within the first 4 weeks of treatment and was suspected to be related to RAD001. Standard antiemetic prophylaxis and anti-hyperlipidemia therapy were allowed. Recruitment was permitted for Cohort 2 if DLTs were observed in 0/3 or $\leq 1/6$ patients in Cohort 1, and for Cohort 3 if DLTs were observed in 0/3 or $\leq 1/6$ patients in Cohort 2. DLTs in $\geq 2/6$ patients in Cohort 1 would result in study discontinuation; DLTs in $\geq 2/6$ patients in Cohort 2 or 3 would result in additional patient enrollment in Cohorts 1 and 2, respectively. The maximum-tolerated dose was defined as the dose at which two or more patients experienced a DLT in the first cycle.

ASSESSMENTS

Blood samples for pharmacokinetic analysis were collected on days 1 and 15 of cycle 1 at 0, 1, 2, 4, 6, 8 and 24 h after RAD001 administration. Blood samples for assessment of the trough concentration (C_{\min}) of RAD001 were obtained immediately before administration of the next dose on days 2, 8, 11, 15 and 16 of cycle 1 and on day 1 of cycle 2 as well as at the end of the study. Pharmacokinetic parameters of RAD001 determined for each cohort included the maximum blood concentration (C_{\max}), time of maximum concentration (t_{\max}), area under the concentration-versus-time curve from time 0 to 24 h after drug administration (AUC_{0-24} , dosing interval) and apparent systemic clearance (CL/F). Drug safety and tolerability were assessed according to the NCI Common Terminology Criteria for Adverse Events (CTCAE) scale, version 3.0. Patients were monitored for adverse events throughout the study. Tumor volume was evaluated every 2 months and at the end of the study according to RECIST. Data were recorded for up to 28 days after discontinuation of treatment.

STATISTICS

The number of patients in each proposed cohort was based on the standard '3 + 3' design for dose-escalation studies. A total of 9–18 patients were planned to assess the safety and tolerability of RAD001, depending on observed toxicities. Descriptive statistics were used for evaluation of safety, efficacy and pharmacokinetic outcomes.

RESULTS

PATIENT CHARACTERISTICS

Between November 2005 and December 2006, nine patients with advanced, refractory solid tumors were enrolled in the study at the two participating centers (Kinki University School of Medicine and National Cancer Center Hospital East) (Table 1). The median age was 64 years (range, 49–74). All patients had received prior chemotherapy for their disease, and most of them had previously undergone cancer-related surgery. The median durations of RAD001 therapy were 57 days in the 2.5 mg/day cohort, 42 days in the 5 mg/day cohort and 98 days in the 10 mg/day cohort. Treatment was discontinued in all nine patients as a result of either progressive disease ($n = 4$), toxicities ($n = 2$), consent withdrawal ($n = 2$) or death ($n = 1$, hemorrhage). All patients were evaluable for drug safety and pharmacokinetics.

SAFETY

DLTs were not observed for any patient in the first cycle of treatment (28 days). Overall, the most common adverse events of all grades were thrombocytopenia (56% of patients), leukopenia (33%), anorexia (44%) and rash (44%) (Table 2). One patient with colon cancer and both lung and liver metastases was treated at the RAD001 dose of 5 mg/day experienced grade 2 pneumonitis after 142 days of therapy. The patient developed cough, and computed tomographic scan of the chest revealed new ground-glass opacities. The patient was hospitalized with PaO_2 of 72.7 mmHg.

Table 1. Patient characteristics

Characteristic	No. of patients
Sex	
Male	4
Female	5
Performance status (ECOG)	
0	5
1	4
Previous therapy	
Surgery	8
Chemotherapy	9
Radiotherapy	3
Tumor type	
Colorectal cancer	3
Lung cancer	3
Esophageal cancer	1
Gastric cancer	1
Thyroid cancer	1

The median (range) age was 64 (49–74) years. ECOG, Eastern Cooperative Oncology Group.

Table 2. Number of patients with adverse events in all courses thought to be attributable to RAD001

Adverse event	RAD001 dose (mg/day)						Total
	2.5 (n = 3)		5 (n = 3)		10 (n = 3)		
	G1/2	G3/4	G1/2	G3/4	G1/2	G3/4	
Thrombocytopenia	0	0	2	0	3	0	5
Leukopenia	1	0	2	0	0	0	3
Neutropenia	1	0	0	0	0	0	1
Anemia	0	0	0	0	1	0	1
Anorexia	1	0	2	0	1	0	4
Rash	0	0	1	0	3	0	4
Stomatitis	1	0	0	0	0	1	2
Nausea	1	0	0	0	1	0	2
Mucosal inflammation	0	0	0	0	2	0	2
Diarrhea	0	0	2	0	0	0	2
Fatigue	0	0	1	0	0	1	2
Weight decreased	1	0	0	0	1	0	2
Elevated ALT or AST	2	0	0	0	0	0	2
Hyperglycemia	0	0	0	0	0	1	1
Hemorrhage	0	0	0	0	0	1	1
Pneumonitis	0	0	1	0	0	0	1
Hypertension	1	0	0	0	0	0	1
Glucose tolerance impaired	0	0	1	0	0	0	1

Includes all adverse events occurring in two or more patients or were \geq Grade 2. G, grade; ALT, alanine aminotransferase; AST, aspartate aminotransferase.

Steroid treatment and discontinuation of RAD001 resulted in marked improvement of the patient within days. All toxicities of Grade 3 or 4 occurred at the dose of 10 mg/day, but none occurred in the first cycle and therefore did not qualify as DLTs. One patient with advanced esophageal carcinoma at a dose of 10 mg/day developed Grade 3 fatigue and stomatitis on day 58 and RAD001 was interrupted. The study drug was restarted on day 66 at a reduced dose of 5 mg/day. On day 71, the patient visited the hospital because of hemorrhage from the right supraclavicular tumor which was a metastatic focus. Although the patient was treated as an inpatient, the Grade 4 hemorrhage could not be controlled and the patient died on day 78. Since RAD001 markedly diminished the size of the patient's metastatic focus, the cause of death was hemorrhage from either the right supraclavicular metastatic focus or the enriched vessels. The study drug did not seem to be the direct cause of hemorrhage. The other two patients in the 10 mg/day cohort took RAD001 for >3 months. One patient with colorectal cancer was treated with 10 mg/day and experienced Grade 3 hyperglycemia on day 98. The patient was determined to have progressive disease on the same day. Another patient in the 10 mg/day cohort

did not have any Grade 3 or 4 toxicities and discontinued RAD001 due to disease progression on day 154.

PHARMACOKINETICS

Pharmacokinetic parameters of RAD001 are summarized in Table 3. The C_{max} of RAD001 was apparent 2 h after administration of a single dose of the oral drug (Table 3 and Fig. 1A). The C_{min} of RAD001 indicated that a steady state was attained after ~ 8 days of repeated once-daily oral dosing (Fig. 1B). Determination of the AUC_{τ} on days 1 and 15 revealed that the exposure to RAD001 achieved after multiple dosing was about twice that achieved after a single

dose (Table 3). On day 1, C_{max} and AUC_{τ} increased almost dose-proportionally. At steady state (day 15), C_{max} and AUC_{τ} increased with increment of dose but dose-proportionality was not clear due to large inter-individual variability in the 5 mg/day cohort.

TUMOR RESPONSE

Among seven patients evaluable for tumor response, obvious tumor shrinkage was observed in two patients treated at the dose level of 10 mg/day. A 60-year-old male with advanced esophageal carcinoma who had been treated with seven prior chemotherapy regimens started treatment with RAD001 at

Table 3. Pharmacokinetic parameters of RAD001

	RAD001 dose (mg/day)		
	2.5 (n = 3)	5 (n = 3)	10 (n = 3)
Day 1			
t_{max} (h)			
Median	1.98	1.00	2.00
Range	0.98–2.00	1.00–1.95	1.92–2.00
C_{max} (ng/ml)	15.1 \pm 2.48	31.5 \pm 3.40	49.4 \pm 14.8
AUC_{τ} (ng h/ml)	85.2 \pm 18.7	211 \pm 50.0	401 \pm 51.6
Day 15			
t_{max} (h)			
Median	1.92	1.98	2.02
Range	1.00–1.98	1.93–1.98	2.00–2.20
C_{max} (ng/ml)	16.8 \pm 1.33	57.6 \pm 17.6	65.9 \pm 14.0
AUC_{τ} (ng h/ml)	134 \pm 24.1	543 \pm 189	711 \pm 113
CL/F (lh)	19.1 \pm 3.26	9.94 \pm 3.21	14.3 \pm 2.23

Data are means \pm SD unless indicated otherwise. t_{max} , time of maximum concentration; C_{max} , maximum blood concentration; AUC_{τ} , area under the concentration-versus-time curve from time 0 to 24 h after drug administration; CL/F, apparent systemic clearance.

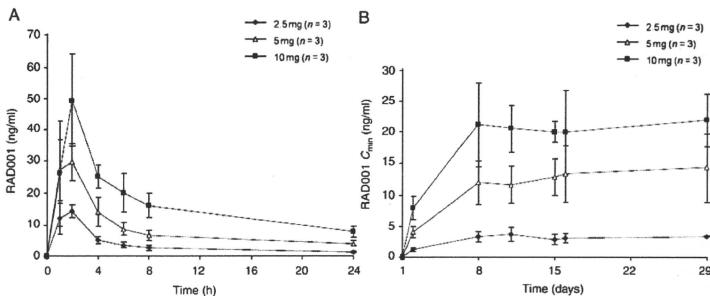


Figure 1. Pharmacokinetics of RAD001. (A) Blood concentration of RAD001 after administration of a single oral dose (2.5, 5 or 10 mg) on day 1 of cycle 1. Data are means \pm SD. (B) Blood trough concentration (C_{min}) of RAD001 during continuous oral dosing for 29 days (cycle 1). Data are means \pm SD.